Journal of Applied Polymer Science

Degradation Behaviors of Perfluorosulfonic Acid Polymer Electrolyte Membranes for Polymer Electrolyte Membrane Fuel Cells Under Varied Acceleration Conditions

Shichun Mu, Cheng Xu, Qing Yuan, Ying Gao, Feng Xu, Pei Zhao
State Key Laboratory of Advanced Technology for Materials Synthesis and Processing, Wuhan University of Technology, Wuhan 430070, China
Correspondence to: S. Mu (E-mail: msc@whut.edu.cn)

ABSTRACT: The degradation of perfluorosulfonic acid (PFSA) membranes (e.g., Nafion membranes) in polymer electrolyte membrane fuel cells has caused wide widespread concern. However, their degradation behaviors, which lead to the damage of fuel cells, need to be investigated under alternative accelerating environments by the simulation of fuel-cell operating conditions. Nafion membranes showed a homogeneous degradation behavior during hydrogen peroxide (H_2O_2) aging, whereas a nonhomogeneous (or crack-type) degradation behavior occurs for Nafion membranes aged in an H_2O_2/Fe^{2+} system (Fenton's reagent), where plenty of the typical microcracks appeared. Interestingly, in the case of nonhomogeneous degradation, the membrane presented a lower fluoride emission rate than that with the homogeneous degradation; this indicates a possible selective attack model of free radicals to both CF_2 and the defect end groups in PFSA membranes. In addition, the effects of the different degradation behaviors on the thermal stability and water uptake of membranes were examined by thermogravimetric analyses. H_2 crossover and single-fuel-cell tests were carried out to evaluate the influence of the degradation behaviors on the fuel-cell performance. These showed that the membrane with a nonhomogeneous degradation behavior had a higher hydrogen crossover and was more destructive than that with a homogeneous behavior. © 2012 Wiley Periodicals, Inc. J. Appl. Polym. Sci. 129: 1586–1592, 2013

KEYWORDS: ion exchangers; ionomers; membranes

Received 4 September 2012; accepted 30 October 2012; published online 18 December 2012
DOI: 10.1002/app.38785

INTRODUCTION

Polymer electrolyte membrane (PEM) fuel cells are promising power sources for the future; however, the durability of PEM fuel cells is one of the most critical issues that needs to be tackled before they are commercialized. Studies have shown that the limited life span of PEM fuel cells is primarily related to the degradation of PEMs under harsh operating conditions.[1,2] The degradation mechanism of various perfluocarbon PEMs, including perfluorosulfonic acid (PFSA) membranes and composite membranes, has been investigated;[3] these studies have indicated that the perfluocarbon PEM can be chemically degraded by a peroxide radical attack mechanism caused by the cross leakage of H_2 and O_2.[4–7] Yu et al.[8] used density functional theory to establish the potential energy surfaces for various plausible reactions involving intermediates and suggested that OH free radicals might be present during the oxygen reduction reaction, especially when fuel cells are turned on and off. In addition, the introduction of trace amounts of divalent metal ions (e.g., Fe^{2+}) into a hydrogen peroxide (H_2O_2) system may accelerate membrane degradation:[4,6,9,10]

$$H_2 \longrightarrow 2H\cdot \text{ (on a Pt catalyst)} \quad (1)$$

$$H + O_2 \text{(diffused through PEM)} \longrightarrow HO_2\cdot \quad (2)$$

$$HO_2\cdot + H^+ \longrightarrow H_2O_2 \quad (3)$$

$$H_2O_2 + M^{2+} \longrightarrow M^{3+} + HO\cdot + OH^- \quad (4)$$

$$H_2O_2 + HO\cdot \longrightarrow HO_2\cdot + H_2O \quad (5)$$

where M is a transition metal with variable valances. The production of H_2O_2 during the oxygen reduction reaction can be measured by the rotating ring–disk electrode technique.[11] The formed OH radical can attack the S—C bond in Nafion and H_2 crossover gas to form H_2SO_4 plus a carbon radical and a hydrogen radical (H·), respectively. The produced H·, which subsequently attacks a C—F bond in Nafion to form HF plus carbon radicals. The products (HF, OCF_2, and SCF_2) of the proposed mechanism were all investigated by F-NMR.[8] Chemical degradation is considered to reduce the chain flexibility, as expressed by smaller motional amplitudes, most probably because of chain

crosslinking.[7] The products of HF by previous radical reactions with PFSA (Nafion) ionomers are listed later:[9]

$$R_f\text{—}CF_2COOH + OH\cdot \longrightarrow R_f\text{—}CF_2 + CO_2 + H_2O \quad (6)$$

$$2R_f\text{—}CF_2 + 2OH\cdot \longrightarrow R_f\text{—}CF_2OH + R_f\text{—}COF + HF \quad (7)$$

$$R_f\text{—}COF + H_2O \longrightarrow R_f\text{—}COOH + HF \quad (8)$$

where R_f is a perflurocarbon group. However, the degradation process of PFSA membranes is rather complicated under real operation conditions in fuel cells; this adds difficulty to the understanding of their degradation behaviors. Few studies have been concerned with the degradation behavior of Nafion membranes under varied accelerating environments and, particularly, its influence on fuel-cell performance. Our previous studies have shown that recast ionomer (Nafion) films in catalyst layers can be degraded by different degradation behaviors in H_2O_2 and H_2O_2/Fe^{2+} (or Fenton's reagent) solutions.[12,13] A Nafion membrane aged chemically in H_2O_2 revealed a homogeneous degradation behavior; on the contrary, a nonhomogeneous degradation behavior resulted in the most important characteristics, that lots of cracks formed, when the membrane was treated in Fenton's reagent. Thus, the degradation of Nafion membranes was worth investigating through their soaking in both H_2O_2 and H_2O_2/Fe^{2+} solutions.

EXPERIMENTAL

Fresh Nafion NRE 211 membrane samples with areas of 5 × 5 cm^2 were soaked in 400 mL of a 30 wt % H_2O_2 solution in a beaker at 70°C in a water bath. The accelerated tests lasted for 50, 100, 200, and 300 h, and H_2O_2 was compensated in time. Subsequently, membrane samples of the same size were soaked in 400 mL of 30 wt % H_2O_2 with 20 ppm Fe^{2+} species (Fenton's reagent) under the same conditions at corresponding time points. All of the membranes were placed transversely along the bottom of the beakers throughout the process.

The aged membranes were observed by scanning electron microscopy (SEM; JSM-5600, JEOL, Tokyo, Japan). For cross-sectional analyses, the dry samples were freeze-fractured in liquid nitrogen. The degradation of the membranes was determined by Fourier transform infrared (FTIR) spectroscopy (Nicolet 170SX, Madison, WI, USA), and the fluoride emission rate (FER) as the macroscopic rate of membrane degradation, which reflects H_2O_2/radical generation,[14,15] was determined with a Dionex DX-600 ion chromatography system (column Ion Pac AS9-HC, 4 mm; Manasquan, New Jersey, USA). Aqueous samples were collected and then filtered through 0.2-μm filters. The filtrate was collected directly into a clean plastic autosampler vial for analyses. Thermogravimetric analysis (TGA; STA 449C, Netzsch Co., Selb, Germany) was used to characterize the thermal stability of the membranes under air flowing at 10 mL/min. The structural integrity of the membranes after acceleration was investigated by hydrogen crossover measurements. Fuel cells assembled with catalyst-coated membranes (CCMs) were operated at 70°C at atmospheric pressure and with an anode/cathode humidity of 100/100% relative humidity. Then, linear sweep voltammetry was used to determine the hydrogen crossover rate through the CCMs in the fuel cells. For the linear sweep voltammetry, the sweep rate was 4 mV/s, and the cell potentials were scanned from 0.01 to 0.05 V to obtain the limiting current (mA/cm^2) according to refs. [13] and [16]. The CCM was prepared by Wilson and Gottesfeld's method.[17] The catalyst ink was coated on the surface of polytetrafluoroethylene membranes to form catalyst layers; after curing, the catalyst layers were then transferred onto both sides of Nafion NRE 211 membranes. The as-prepared CCM had a Pt loading of about 0.4 mg/cm^2. To test the performance degradation of fuel cells with various membrane samples, single fuel cells with active areas of 25 cm^2 were adopted. H_2/air (1.5 : 2) with 100% humidity was used as the reaction gas, and the cell temperature was 70°C at atmospheric back pressure.

RESULTS AND DISCUSSION

As shown in Figure 1(A), the pristine Nafion membrane surfaces were smooth, and no visible flaws were observed. The membrane treated for 50 h in the H_2O_2 system [Figure 1(B)] revealed almost the same morphological feature as that of the raw membrane. Subsequently, a few small white humps related to microbubbles in the membrane surfaces occurred after 100 h of treatment [Figure 1(C)] and expanded further onto the entire membrane surface after 200 and 300 h [Figure 1(D–F)]. However, destructive structures, including obvious microcracks, were not observed during the 300-h treatments [Figure 1(F)]. There appeared to be thin layers in white or light gray on both sides of the membrane with section thicknesses of 3–4 μm [Figure 1(G)] compared to that of the pristine membrane [Figure 1(H)]. These changes may have been caused by the previously discussed humps.

Some small humps with a few microcracks were observed in the membrane surfaces after chemical aging in Fenton's reagent system for 50 h [Figure 2(A)]. However, to our surprise, a large number of round humps with increased microcracks caused by microbubble breaking occurred after 100 h of treatment in Fenton's reagent [Figure 2(B)]. It was very interesting that these microcracks primarily occupied the central location of the microbubbles and gradually expanded onto the edges. The amount of microcracks increased with Fenton's reagent treatments from 200 to 300 h [Figure 2(C,D)]. However, it should be pointed out that a substantial quantity of microbubbles ceased to develop with time. As shown in Figure 1(E,F), the cross-sections of the membranes presented this radical change in the structural properties compared with that of samples tested in H_2O_2. The amount and size of microcracks increased with Fenton's reagent treatments from 50 to 300 h. We believe that microcracks may further develop into pinholes with aging and led to the failure of fuel cells due to a strong hydrogen crossover effect.

The reflectance FTIR spectroscopy was used to investigate the surface characteristics of the membrane materials.[12,13,18] Figure 3(A,B) shows the reflectance FTIR spectra of the Nafion membranes before and after degradation. The main stretching bands were identified by previous studies[19–21] (see Table I). As shown in Figure 3(A), the stretching intensities of CF_2 at 1207 and 1149 cm^{-1} visibly decreased with acceleration; this indicated that the CF_2 group of Nafion was attacked by peroxide radicals,

Applied Polymer SCIENCE

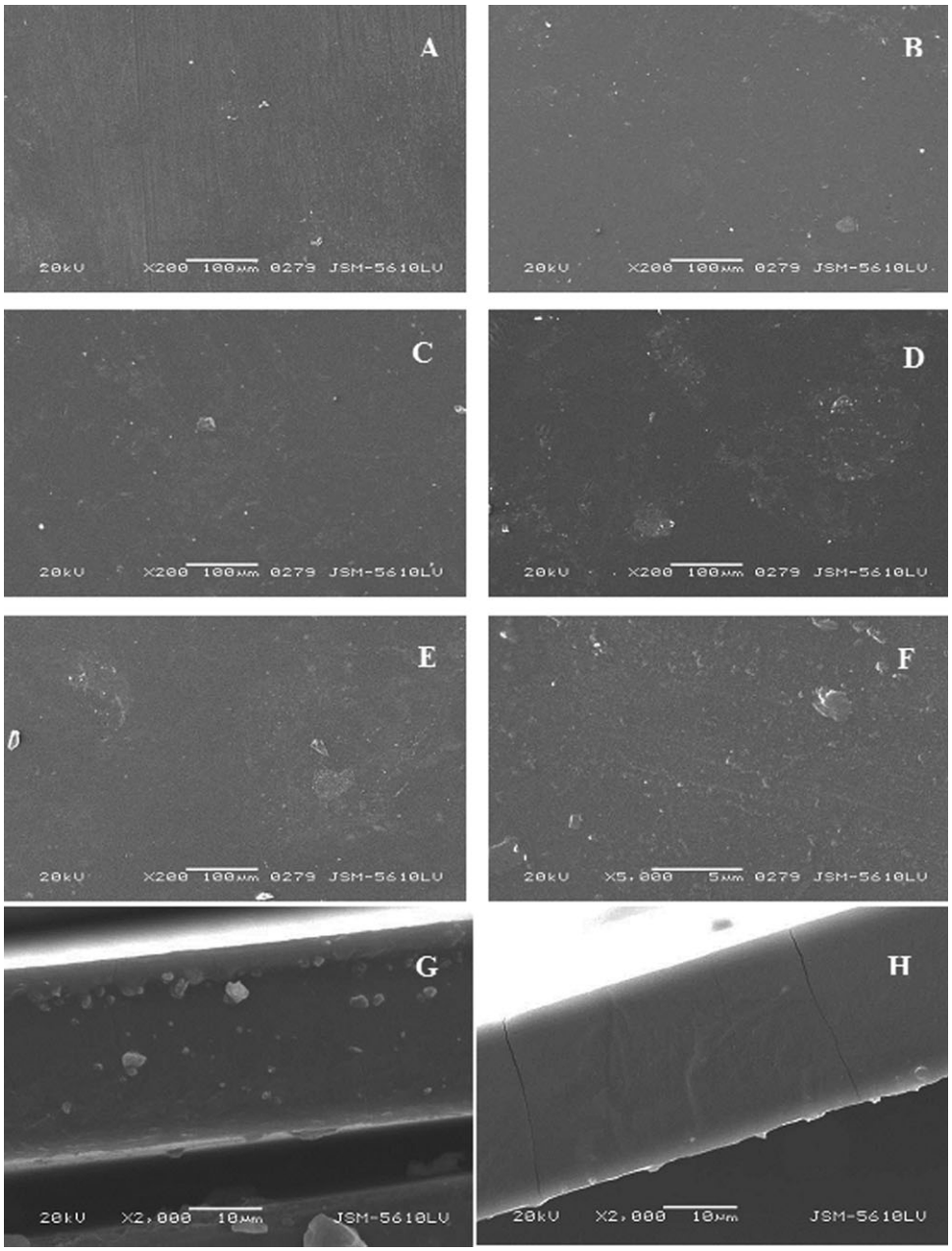

Figure 1. SEM images of the H_2O_2-treated Nafion membranes: (A) pristine membrane, (B) membrane treated for 50 h, (C) membrane treated for 100 h, (D) membrane treated for 200 h, (E) membrane treated for 300 h, (F) an enlargement of image E, (G) 300 h (cross section), and (H) pristine membrane (cross section).

and this led to fluoride emission.[10] This was in accordance with a conclusion by Curtin et al.,[9] where they reported that Nafion degradation began in the CF_2 end groups. In addition, the homogeneous decrease in the stretching intensity of CF_2 may have showed a uniform degradation of CF_2 during acceleration. Figure 3(B) also shows a visible decrease in the stretching bands of CF_2 at 1207 and 1145 cm^{-1}. However, this change was not homogeneous. The rapid degradation of Nafion occurred in the ranges of 0–100 and 200–300 h, respectively; this indicated a very varied degradation behavior of the Nafion membranes in the H_2O_2 and H_2O_2/Fe^{2+} systems, respectively. The H_2O_2-treated sample showed a homogeneous degradation behavior, whereas a nonhomogeneous (or crack-type) degradation behavior was revealed in the H_2O_2/Fe^{2+} treated sample.

We tend to suspect that a visible inactivation took places during the 100–200-h treatments in H_2O_2/Fe^{2+}. Figure 4 demonstrates the inactivation region of degradation during the 100–200-h treatments and an increased degradation region during the 0–100- and 200–300-h treatments characterized by FER in solutions. Nafion degradation rapidly increased in the case of H_2O_2 treatments, whereas a slow release of fluorite occured in the Fenton's reagent treated samples. These revealed that the H_2O_2-treated membrane had a higher degradation rate than the

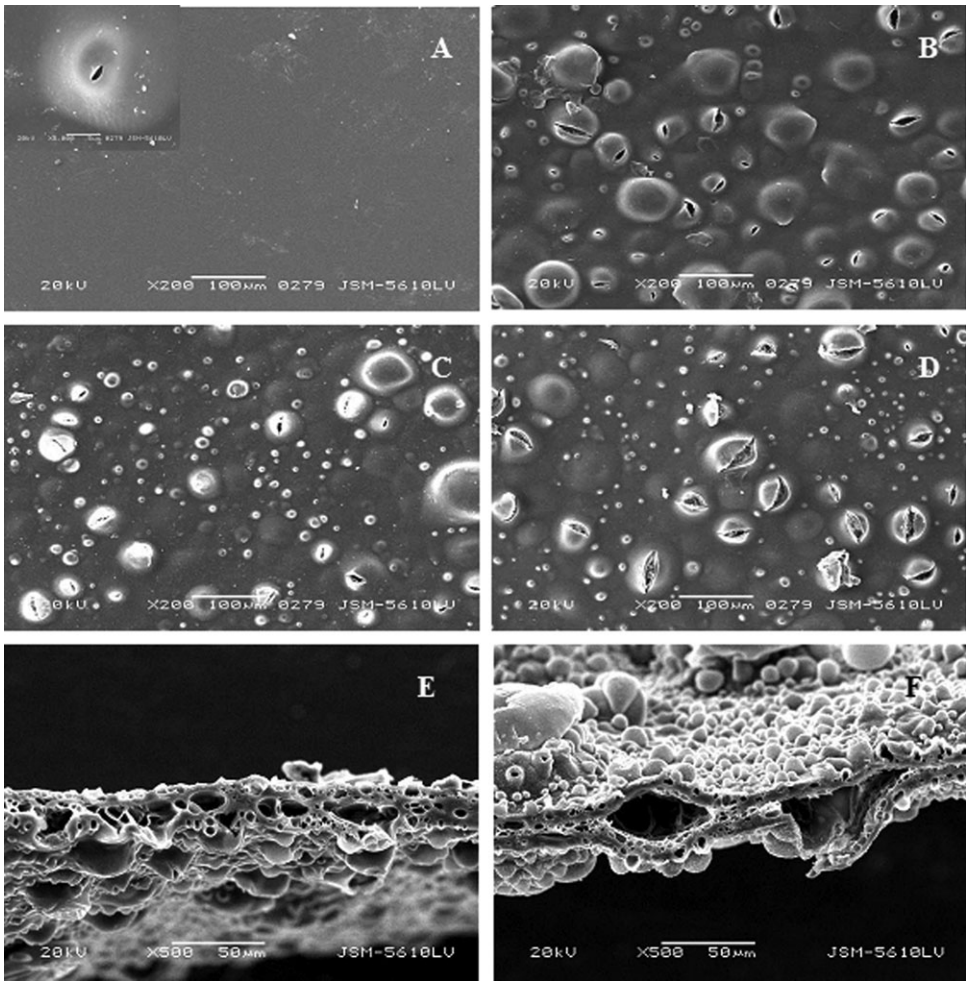

Figure 2. SEM images of the H_2O_2/Fe^{2+}-treated Nafion membranes treated for (A) 50 h (the upper left is an enlargement of one special location in the image), (B) 100 h, (C) 200 h, (D) 300 h, (E) 50 h (cross section), and (F) 300 h (cross section).

Fenton's reagent treated membrane; this was consistent with our previous study of Nafion film degradation in catalyst layers.[12,13]

Pozio et al.[10] discussed the mechanism of the introduced Fe^{2+} in the degradation of Nafion membranes. They believed that Fe^{2+} or Fe^{3+} could combine with Nafion molecules and promote Nafion degradation as follows:

$$\text{Nafion}-Fe^{2+} + H_2O_2 \longrightarrow \text{Nafion}-Fe^{3+} + HO\cdot + OH^- \quad (9)$$

$$\text{Nafion}-Fe^{3+} + H_2O_2 \longrightarrow \text{Nafion}-Fe^{2+} + HO_2 + H^+ \quad (10)$$

If this point of view is correct, the degradation of Nafion membranes in Fenton's reagent should be homogeneous, the same as that in H_2O_2. However, this result was inconsistent with our previous findings by both SEM and FTIR spectroscopy. Considering the presence of nonuniform defect end groups (especially carboxylic end groups) in commercialized Nafion membranes, which are responsible for fluoride ion radicals,[7,22] we suggest a selective attack model of free radicals to CF_2 end groups and defect end groups. The formed $HO_2\cdot$ in eqs. (2), (5), and (10) tended to attack various parts of the Nafion molecular chains in addition to the defect end groups without selectivity; consequently, a homogeneous degradation behavior for H_2O_2-treated Nafion membranes is observed. This result may well explain why microbubbles uniformly occur in the membranes. Instead, the initially produced ·OH in eqs. (4) and (9) possibly takes a fixed-point attack to carboxylic acid end groups in Nafion; this indicates a nonhomogeneous degradation behavior due to the nonuniform distribution of defect end groups. This may give us a preliminary interpretation regarding only some particular microbubbles that grow into microcracks in H_2O_2/Fe^{2+}-treated membranes.

Generally, perfluorinated Nafion exhibits at least three thermal decomposition stages according to TGA.[23,24] The first stage (50–180°C) is related to a loss of moisture in the membranes. The second stage (290–420°C) corresponds to the decomposition of SO_3 groups. The third stage, at the late 420°C, is assigned to the decomposition of the perfluorinated matrix. However, Deng et al.[25] considered that the end of the second stage should be at 470°C. Figure 5(A) shows the thermal stability of the H_2O_2-treated membranes as determined by TGA. The weight loss of membranes at temperatures below 180°C was less than that of the original membranes. A slight weight loss observed in the

Applied Polymer SCIENCE

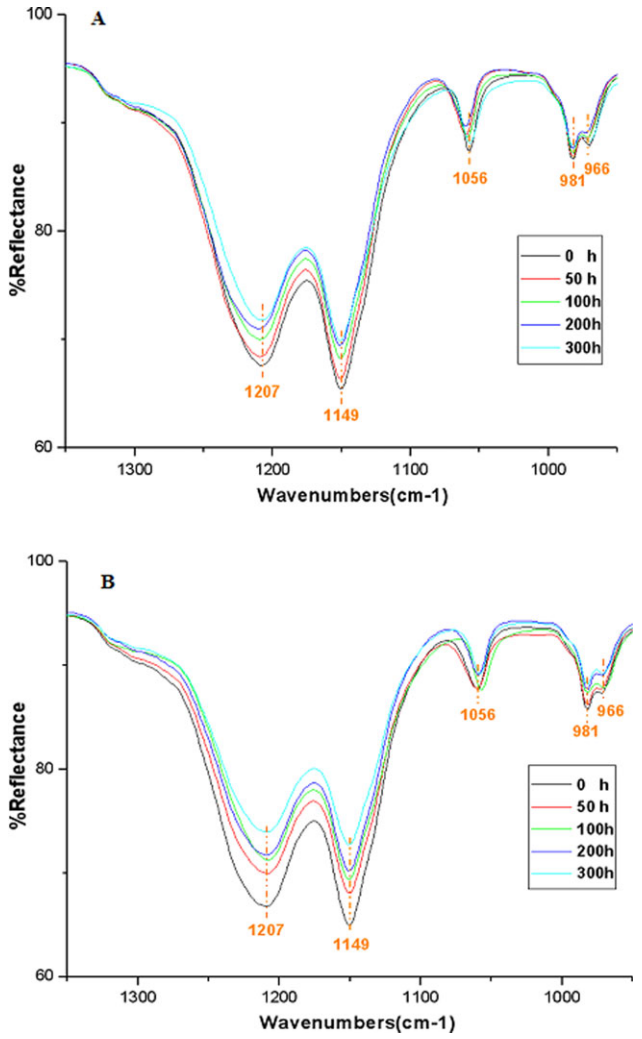

Figure 3. FTIR spectra of the Nafion membranes in (A) H_2O_2 and (B) H_2O_2/Fe^{2+} with various accelerated time. [Color figure can be viewed in the online issue, which is available at wileyonlinelibrary.com.]

second stage for the H_2O_2-treated membranes revealed that the sulfonic group (SO_3H) could almost remain stable even though it was attacked by free radicals. At the late 420°C, the T_g slope decreased compared to that of the original membranes because of the decomposition of perfluorinated matrix.

Figure 5(B) shows an increased weight loss for the H_2O_2/Fe^{2+}-treated membranes at temperature below 180°C. We assumed

Table I. Selected IR Absorption Bands of Nafion

Band location (cm^{-1})	Assignment
~1201	CF_2 stretching, asymmetric
~1145	CF_2 stretching, symmetric
~1056 s	S—O stretching, symmetric
~981 s	C—F stretching [—CF_2—$CF(CF_3)$—group]
~966 s	C—O—C stretching, symmetric

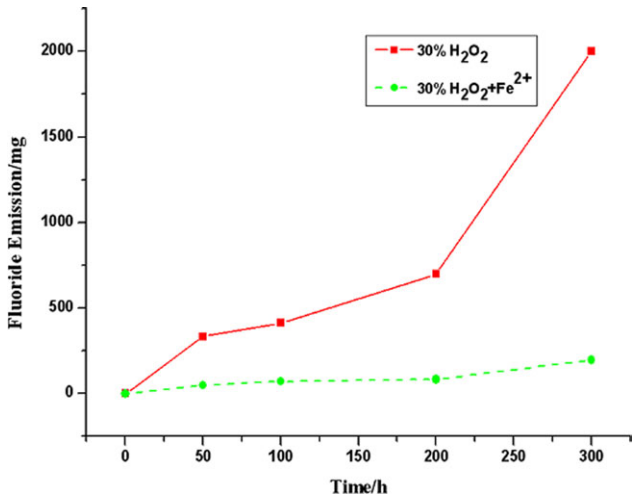

Figure 4. FER of the Nafion membranes degraded under different conditions with time. [Color figure can be viewed in the online issue, which is available at wileyonlinelibrary.com.]

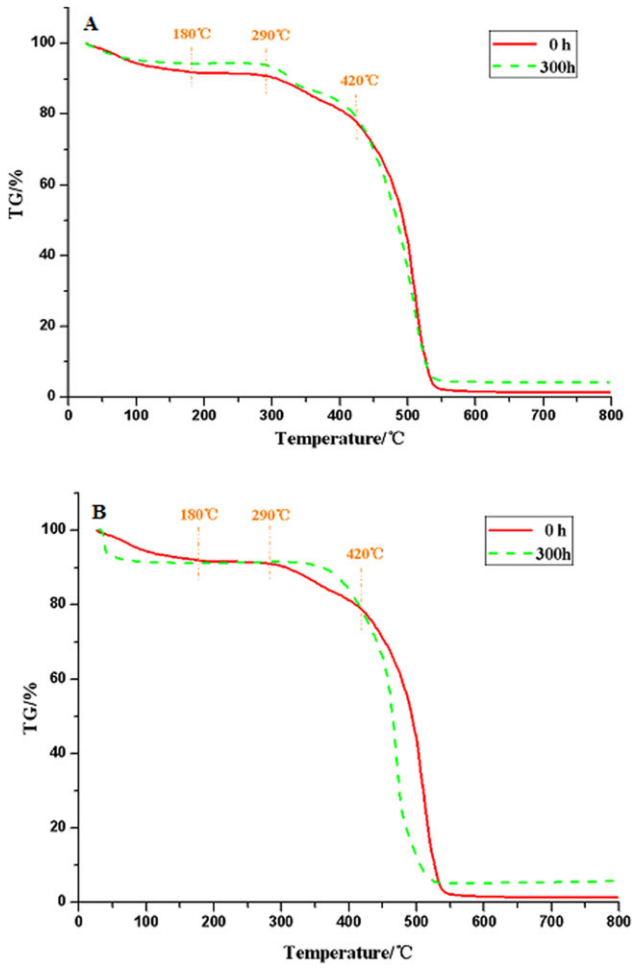

Figure 5. TGA curves of the Nafion membranes as treated in (A) H_2O_2 and (B) H_2O_2/Fe^{2+} with time. [Color figure can be viewed in the online issue, which is available at wileyonlinelibrary.com.]

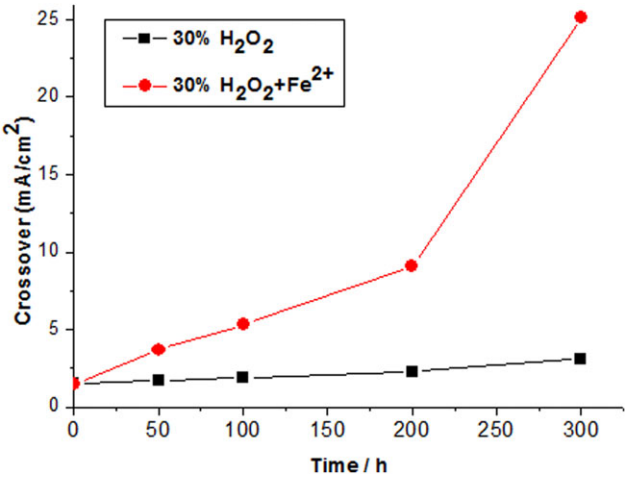

Figure 6. Measured hydrogen crossover by a limiting current during 300 h of accelerated aging. [Color figure can be viewed in the online issue, which is available at wileyonlinelibrary.com.]

that the presence of microcracks increased the specific area of the membranes and led to an enhanced water uptake. An almost identical weight loss was found in the second stage for both the original and treated membranes; this revealed a high stability for SO_3H in the radicals. After 420°C, the T_g slope decreased significantly; this showed an increased decomposition of the perfluorinated matrix, which was related to the growth of microcracks in particular microbubbles.

The formed microcracks could gradually diffuse onto the membranes; this would cause a great destruction to the membrane structural integrity and lead to a profound performance loss in fuel cells. The destruction of these microcracks can be confirmed by hydrogen crossover with voltammetric measurements on fuel cells. As shown in Figure 6, in the case of the H_2O_2/Fe^{2+} treatment, the hydrogen crossover of fuel cells assembled with aged membranes rapidly increased during 300 h of acceleration compared to that of the H_2O_2-aged membrane containing cells at the same accelerated time. The rapid increases of the hydrogen crossover were attributed to the formation of microcracks or pinholes in the PEMs.

Figure 7 shows the fuel-cell performance of various Nafion membrane samples after accelerated aging from 0 to 100 h. Compared with those of the pristine membrane, the open-circuit voltage (OCV) and performance of the fuel cells of the membrane treated by H_2O_2 for 50 h only fell by 0.037 and 0.029 V at 0.6 mA/cm^2, respectively. In contrast, these values of the membrane treated by H_2O_2/Fe^{2+} for 50 h decreased by 0.165 and 0.173 V, respectively. The obvious decrease in the electrochemical performance of the cells with membranes due to H_2O_2/Fe^{2+} treatment was mainly attributed to the hydrogen crossover caused by the microcracks. Subsequently, after 100 h of treatment, a heavy loss of OCV (0.307 V) was observed, and this led to almost no performance output compared to both the pristine and H_2O_2-treated samples. Instead, losses of OCV (0.117 V) and performance (ca. 0.1 V) at 0.6 mA/cm^2 for the H_2O_2-treated sample were present; these indicated a relative low hydrogen crossover due to small amounts of microcracks in the membranes. These results showed that the nonhomogeneous (or crack-type) degradation behavior of the membrane treated by H_2O_2/Fe^{2+} was more destructive for fuel cells than the homogeneous degradation behavior of the membrane caused by H_2O_2; this was in better agreement with the experimental data of the hydrogen crossover.

CONCLUSIONS

The degradation behaviors of Nafion membranes in H_2O_2 with and without Fe^{2+} were evaluated by the simulation of PEM fuel-cell operation conditions. As a result, the membranes show homogeneous and nonhomogeneous (or crack-type) degradation behaviors, respectively, when they were aged in H_2O_2 and H_2O_2/Fe^{2+} systems. Also, a wide range of microcracks in the membranes due to H_2O_2/Fe^{2+} treatment enhanced the water uptake; however, they increased the hydrogen crossover and led to a decrease in OCV and greatly shortened the PEM fuel-cell life span. We primarily supposed a selective attack model of free radicals to Nafion that accounted for the uniform occurrence of microbubbles in membranes in the H_2O_2 system, and only some particular microbubbles grew into microcracks in the H_2O_2/Fe^{2+} system. This research may promote the

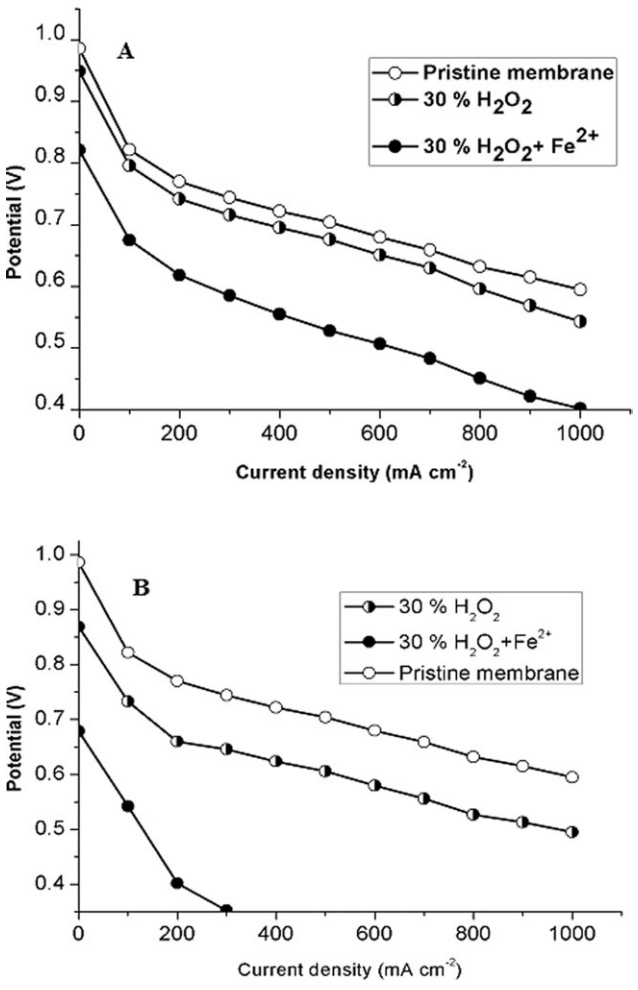

Figure 7. Single-fuel-cell performances of various membrane samples treated for (A) 50 and (B) 100 h.

understanding of Nafion membrane degradation behaviors and their destruction in real fuel cells.

ACKNOWLEDGMENTS

Financial support by the National Natural Science Foundation of China (contract grant number 50972112) and the Major State Basic Research Development Program of China (973 Program; contract grant number 2012CB215500) are gratefully acknowledged.

REFERENCES

1. Wu, J. F.; Yuan, X. Z.; Martin, J. J.; Wang, H. J.; Zhang, J. J.; Shen, J.; Wu, S. H.; Merida, W. J. *Power Sources* **2008**, *184*, 104.
2. Collier, A.; Wang, H. J.; Yuan, X. Z.; Zhang. J. J.; Wilkinson, D. P. *Int. J. Hydrogen Energy* **2006**, *31*, 1838.
3. Tang, H. L.; Pan, M. F.; Wang, J. *Appl. Polym. Sci.* **2008**, *109*, 2671.
4. LaConti, A. B.; Hamdan, M.; McDonal, R. C. Handbook of Fuel Cells: Fundamentals, Technology, and Applications; Vol. *3*; Vielstich, W., Lamm, A., Gasteiger, H. A., Eds.; Wiley: New York, **2003**.
5. Guo, Q.; Pintauro, P. N.; Tang, H.; O'Connor, S. *J. Membr. Sci.* **1999**, *154*, 175.
6. Aoki, M.; Uchida, H.; Masahiro, W. *Electrochem. Commun.* **2006**, *8*, 1509.
7. Ghassemzadeh, L.; Kreuer, K.; Maier, J.; Müller, K. *J. Phys. Chem. C* **2010**, *114*, 14635.
8. Yu, T. H.; Sha, Y.; Liu, W. G.; Merinov, B. V.; Shirvanian, P.; Goddard, W. A. *J. Am. Chem. Soc.* **2011**, *133*, 19857.
9. Curtin, D. E.; Lousenberg, R. R.; Henry, T. J.; Tangeman, P. C.; Tisack, M. E. J. *Power Sources* **2004**, *131*, 41.
10. Pozio, A.; Silva, R. F.; Francesco, M. D.; Giorgi, L. *Electrochim. Acta* **2003**, *48*, 1543.
11. Sethuraman, V. A.; Weidner, J. W.; Haug, A. T.; Motupally, S.; Protsailo, L. V. *J. Electrochem. Soc.* **2008**, *155*, B50.
12. Mu, S. C.; Xu, C.; Gao, Y.; Tang, H. L.; Pan, M. *Int. J Hydrogen Energy* **2010**, *35*, 2872.
13. Mu, S. C.; Zhao, P.; Xu, C.; Gao, Y.; Pan, M. *Int. J Hydrogen Energy* **2010**, *35*, 8155.
14. Marcinkoski, J.; Kopasz, J. P.; Benjamin, T. G. *Int. J. Hydrogen Energy* **2008**, *33*, 3894.
15. Trogadas, P.; Parrondo, J.; Mijangos, F.; Ramani, V. J. *Mater. Chem.* **2011**, *21*, 19381.
16. Bi, W.; Gray, G.E.; Fuller, T. F. *Electrochem. Solid-State Lett.* **2007**, *10*, B101.
17. Wilson, M. S.; Gottesfeld, S. *J. Electrochem. Soc.* **1992**, *139*, 28.
18. Howe, K. J.; Ishida, K. P.; Clark, M. M. *Desalination* **2002**, *147*, 251.
19. Liang, Z. X.; Chen, W. M.; Liu, J. G.; Wang, S. L.; Zhou, Z. H.; Li, W. Z.; Sun, G.Q.; Xin, Q. *J. Membr. Sci.* **2004**, *39*, 233.
20. Ostrovskii, D.; Paronen, M.; Sundholm, F.; Torell, L. M. *Solid State Ionics* **1999**, *116*, 301.
21. Ludvigsson, M.; Lindgren, J.; Tegenfeldt, J. Electrochim. *Acta* **2000**, *45*, 2267.
22. Ohama, A.; Suga, S.; Yamamoto, S.; Shinohara, K. *J. Electrochem. Soc.* **2007**, *54*, B757.
23. Surowiec, J.; Bogoczek, R. *J. Therm. Anal. Calorim.* **1988**, *33*, 1097.
24. Babu, K. S.; Vijayan, C.; Haridoss, P. *Mater. Res. Bull.* **2007**, *42*, 42996.
25. Deng, C.; Wilkie, A.; Moore, R. B.; Mauritz, K. A. *Polymer* **1998**, *39*, 5961.